Electronic Supplementary Information (ESI)

A new 3D four-fold interpenetrated dia-like luminescent Zn(II)-based metal-organic framework: sensitive detection of Fe^{3+}, $Cr_2O_7^{2-}$, CrO_4^{2-} in water and nitrobenzene in ethanol

Tian-Yang Xu[b], Jia-Ming Li[a*], Ya-Hui Han[c], Ai-Rong Wang[a], Kun-huanHe[a], Zhong-Feng Shi[a,b*]

[a] Guangxi Colleges and Universities Key Laboratory of Beibu Gulf Oil and Natural Gas Resource Effective Utilization, College of Petroleum and Chemical Engineering, Beibu Gulf University, Qinzhou 535011, P. R. China

[b] School of Chemistry and Pharmacy, Guangxi Normal University, Key Laboratory for the Chemistry and Molecular Engineering of Medicinal Resources (Ministry of Education), Guilin 541004 People's Republic of China

[c]Sichuan Vocational College of Chemical Technology, Luzhou 646000, P. R. China

[*]Corresponding authors: Jia-Ming Li, e-mail: jmli@bbgu.edu.cn; Zhong-Feng Shi, e-mail: shizhongfeng01@163.com

Table S1. Crystal data and structure refinement for 1.

empirical formula	$C_{56}H_{42}N_{10}O_{12}Zn_2$
formula weight	1177.73
temperature/K	296.15
crystal system	monoclinic
space group	$P2_1/n$
a/Å	13.1992(19)
b/Å	9.2011(9)
c/Å	23.622(2)
β/°	91.877(11)
V/Å^3	2867.2(6)
Z	2
ρ_{calc} g/cm^3	1.364
μ/mm^{-1}	0.905
F(000)	1208.0
crystal size/mm^3	0.25 × 0.18 × 0.12
radiation	Mo Kα (λ = 0.71073)
2θrange for data collection/°	4.752 to 50.198
index ranges	h =± 15, k =±10, -10 ≤ l ≤ 28
reflections collected	10443
independent reflections	5079 [R_{int} = 0.0486, R_{sigma} = 0.0778]
data/restraints/parameters	5079/0/361
goodness-of-fit on F^2	1.085
final R indexes [I>=2σ (I)]	R_1 = 0.0574, wR_2 = 0.1384
final R indexes [all data]	R_1 = 0.0875, wR_2 = 0.1698
largest diff. peak/hole / e Å^{-3}	0.82/-0.85

[a] $R1 = \Sigma||F_o| - |F_c||/\Sigma|F_o|$; [b] $wR_2 = [\Sigma w(F_o^2 - F_c^2)^2/\Sigma w(F_o^2)^2]^{1/2}$

Table S2. Selected bond lengths (Å) and angles (º) for 1.

Zn1-O1	1.971(3)	C7-N1	1.473(6)
Zn1-O4^{i}	2.001(3)	C28-C27	1.347(6)
Zn1-N5^{ii}	1.993(4)	N1-O5	1.248(7)
Zn1-N2	2.006(4)	N1-O6	1.207(6)
O1-C1	1.262(5)	N3-C15	1.323(6)
O4-C14	1.277(6)	N3-C18	1.471(6)
O2-C1	1.242(5)	N3-C17	1.346(8)
O3-C14	1.246(6)	N4-C26	1.337(5)
O1-Zn1-O4^{i}	100.51(13)	C26-N5-Zn1^{iv}	123.4(3)
O1-Zn1-N5^{ii}	105.92(15)	C26-N5-C27	105.8(4)
O1-Zn1-N2	108.31(15)	C27-N5-Zn1^{4}	130.7(3)
O4^{i}-Zn1-N2	113.51(16)	C15-N2-Zn1	127.7(4)
N5^{ii}-Zn1-O4^{i}	111.40(14)	C15-N2-C16	104.0(5)
N5^{ii}-Zn1-N2	115.70(16)	C16-N2-Zn1	128.1(4)
C1-O1-Zn1	117.6(3)	C14-O4-Zn1^{iii}	104.6(3)

Symmetry codes: ^{i}0.5+*x*, 0.5-*y*, 0.5+*z*; ^{ii} -0.5+*x*, 1.5-*y*, 0.5+*z*; ^{iii} -0.5+*x*, 0.5-*y*, -0.5+*z*; ^{iv}0.5+*x*, 1.5-*y*, -0.5+*z*.

Table S3. Hydrogen bonds (Å, °) for 1.

D-H···A	**D-H**	**H···A**	**D···A**	**D-H···A**
C28-H28···O2^{v}	0.93	2.50	3.247(5)	138.1
C15-H15···O2	0.93	2.37	3.094(6)	134.2
C9-H9···O6^{vi}	0.93	2.51	3.236(6)	135.4

Symmetry codes: ^{v} 1.5-*x*, -0.5+*y*, 1.5-*z*; ^{vi} *x*, -1+*y*, *z*.

Table S4. HOMO and LUMO energies for calculated NEs at B3LYP/6-31G(d,p) level of theory.

Analytes	HOMO (ev)	LUMO (ev)	Bond gap
2-nitroanisole	-6.76	-2.16	4.60
p-nitrophenol	-5.87	-2.04	3.83
TNP	-6.92	-2.22	4.70
o-nitrophenol	-6.78	-2.39	4.39
nitrobenzene	-7.60	-2.43	5.17
o-nitroacetophenone	-5.88	-2.12	3.76
(2-nitrovinyl)benzene	-5.85	-2.08	3.77
4,4'-H_2nba	-7.04	-1.94	5.10
1,4-bib	-6.14	-0.76	5.38

Table S5. Comparison of detection capacities of 1 towards Fe3+ ion with other materials.

Materials	Solvent	$K_{sv}(M^{-1})$	Detection limit (μm)	Ref.
$[Eu(atpt)_{1.5}(phen)(H_2O)]_n$	ethanol	7.60×10^3	45	1
$[Cd(L)_2(H_2O)_2]\cdot 2H_2O$	water	7.39×10^3	-	2
$[Eu(HL)_{1.5}(H_2O)(DMF)]\cdot 2H_2O$	water	1.0×10^4	1.03	3
$[Tb(HL)_{1.5}(H_2O)(DMF)]\cdot 2H_2O$	water	9.92×10^3	1.04	3
$[(CH_3)2NH_2]\cdot[Tb(bptc)]$	ethanol	-	180.1	4
Benzimidazole-based sensor	water	8.51×10^4	2	5
1	water	1.68×10^4	1.76	This work

Table S6. Comparison of detection capacities of 1 towards nitrobenzene with other materials.

Materials	Solvent	$K_{sv}(M^{-1})$	Detection limit	Ref.
DF	THF	-	100ppm	6
BDS	THF	-	50ppm	6
$[Cd_2IJL)IJDMA)]\cdot H_2NIJMe)_2$	DMA	2.7×10^3	2.54×10^{-3}M	7
$Zn_3(L1)_2(L2)_{3.6}$ DMF·$4H_2O$	DMF	-	150ppm	8
$Zn_3(L1)_2(L2)$	DMF	-	50ppm	8
$[Cd_2L(H_2O)_2]\cdot DMF\cdot H_2O$	DMAC	-	50ppm	9
$[Cd_2(DTP)_2(bibp)_{1.5}]_n$	DMA	-	60ppm	10
1	ethanol	1.59×10^4	19ppm	This work

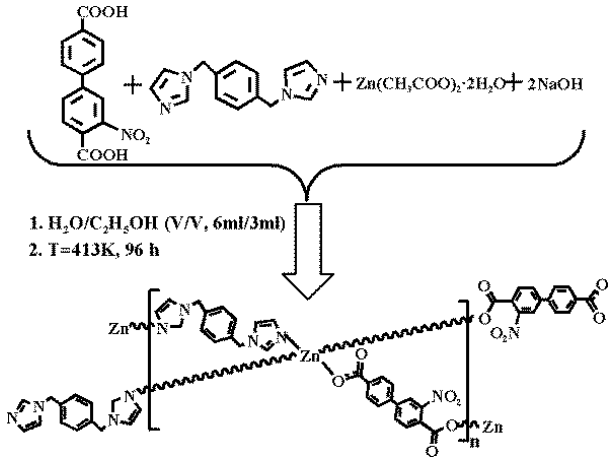

(a)

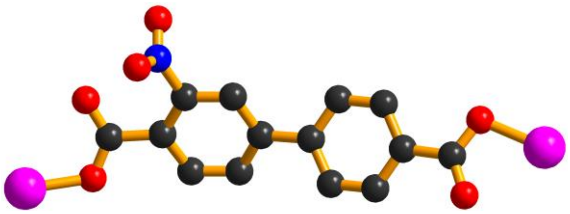

(b)

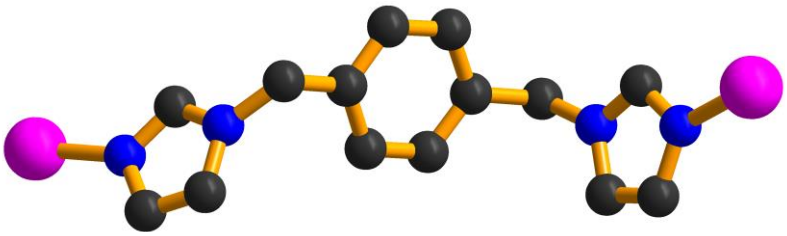

(c)

Scheme S1. (a) The synthesis for **1**. (b) View of the coordination mode of the 4,4′-nba^{2-} ligand in **1**. (c) View of the coordination mode of the 1,4-bib.

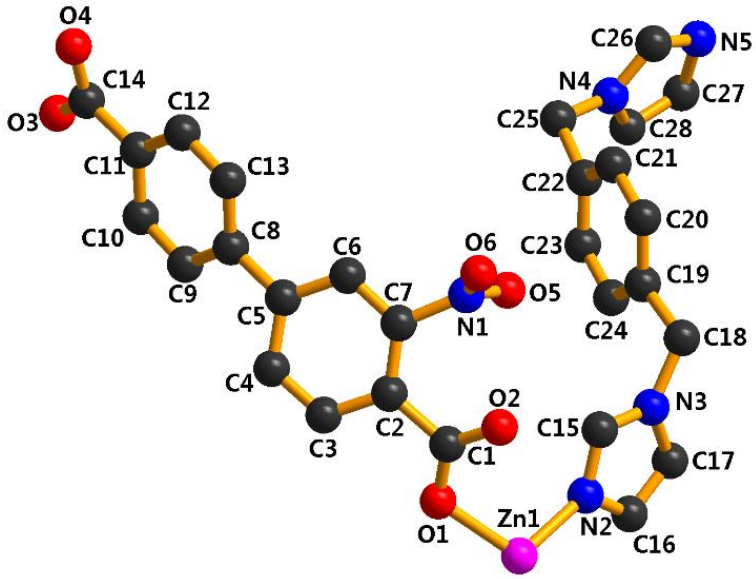

(a)

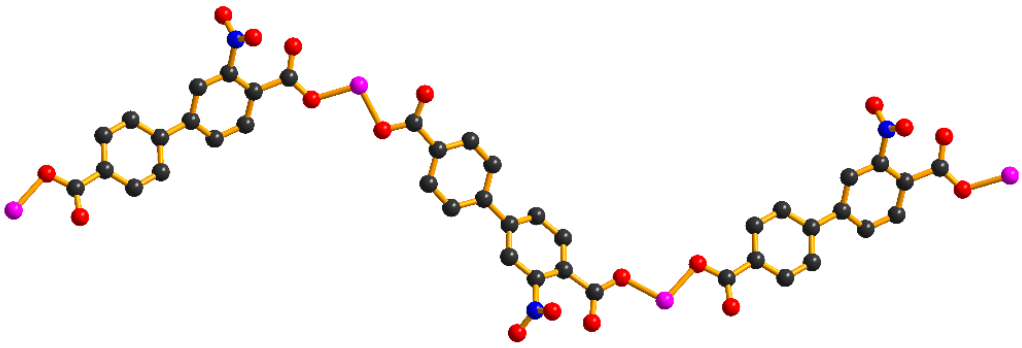

(b)

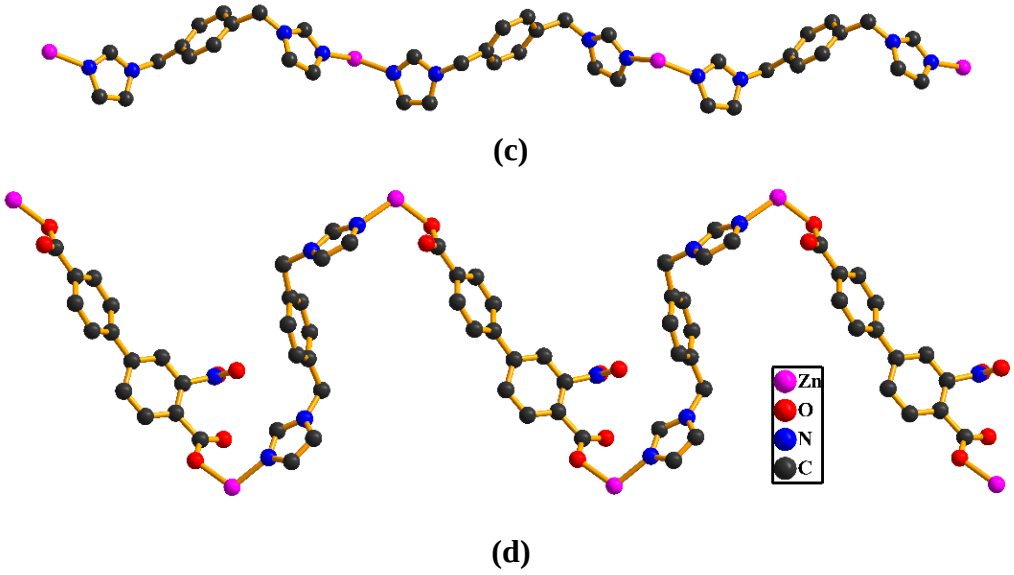

Figure S1. (a) The asymmetric unit of **1**. (b) The wave-shaped 1D chains Zn-4,4′-nba^{2-}. (c) The wave-shaped 1D chains Zn-1,4-bib. (d) The wave-shaped 1D chains 1,4-bib-Zn-4,4′-nba^{2-}.

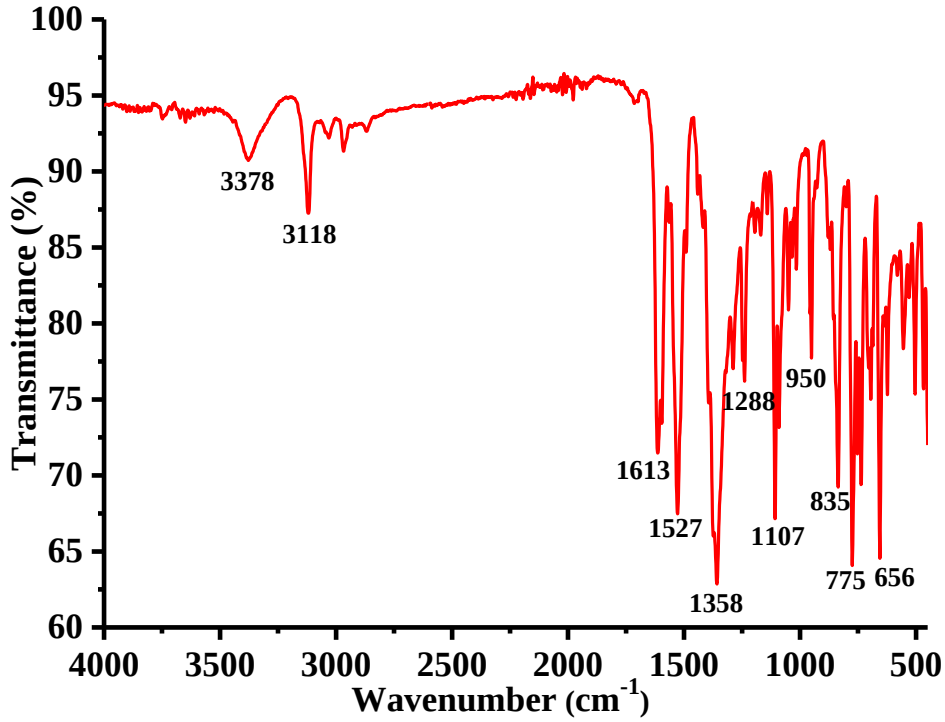

Figure S2. The IR spectra of **1**.

Thermogravimetric analyses of 1

In order to determine the thermal stability of **1**, TG studies have been performed in a nitrogen atmosphere at a heating rate of 10 °C min^{-1}between 20 and 950 °C. For compound **1**, a weight loss of 3.10% was observed in the region 167–212 °C, which is attributed to the severely disordered solvent molecules. After 313 °C, a series of complicated weight losses were also observed as the temperature increased until heating ends (Figure S3).

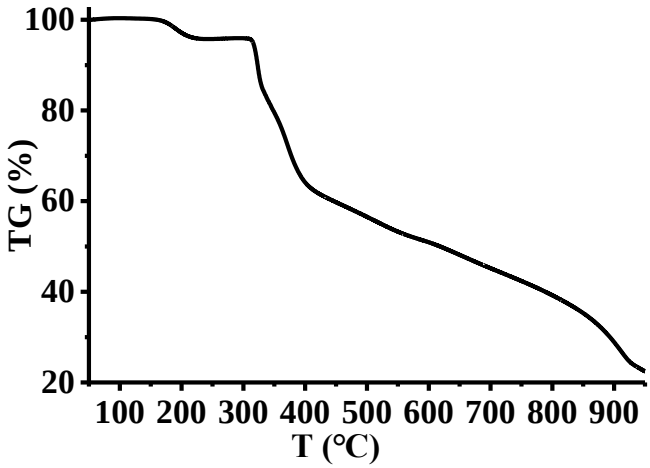

Figure S3. The TG curves for **1**.

The solid-state luminescent properties of 1

Metal-organic coordination complexes constructed from d^{10} metal atoms (or d^{10} metal clusters) (such as Zn^{2+}, Cd^{2+} and Hg^{2+}) and conjugated organic ligands have attracted great interest because of their various potential applications in chemical sensors, photochemistry, and electroluminescent displays.[11,12]The solid-state luminescent excitation and emission spectra of 4,4′-H_2nba, 1,4-bib and **1** were recorded at room temperature. As shown in Figure S4, the strongest excitation peaks for the free 4,4′-H_2nba and 1,4-bib are at 374 and 396 nm,and their emission spectra mainly show the strongest peaks at 423 and 471nm, respectively, which is attributed to the π*→n or π*→π electronic transitions.[11] The strongest emission peak for **1** is at 423nm with the excitation peak at

374nm, which may chiefly originate from ligand-centered electronic transitions perturbed by the coordination to mental ions.[12] In compared with the excitation and emission of the free 4,4′-H_2nba, 1,4-bib and **1**, the free 4,4′-H_2nba and **1**show a similar spectrashape except the intensities but adistinct differenceof the 1,4-bib with the biggest emission peak at a red-shift of about 48nm. Since the Zn^{2+} ion is difficult to oxidize or to reduce due to its d^{10} configuration, and the profile of the emission band is quite similar to that of the free 4,4′-H_2nba ligand except the intensities, the emission of **1** could be attributed to intrigant (π–π*) emission.

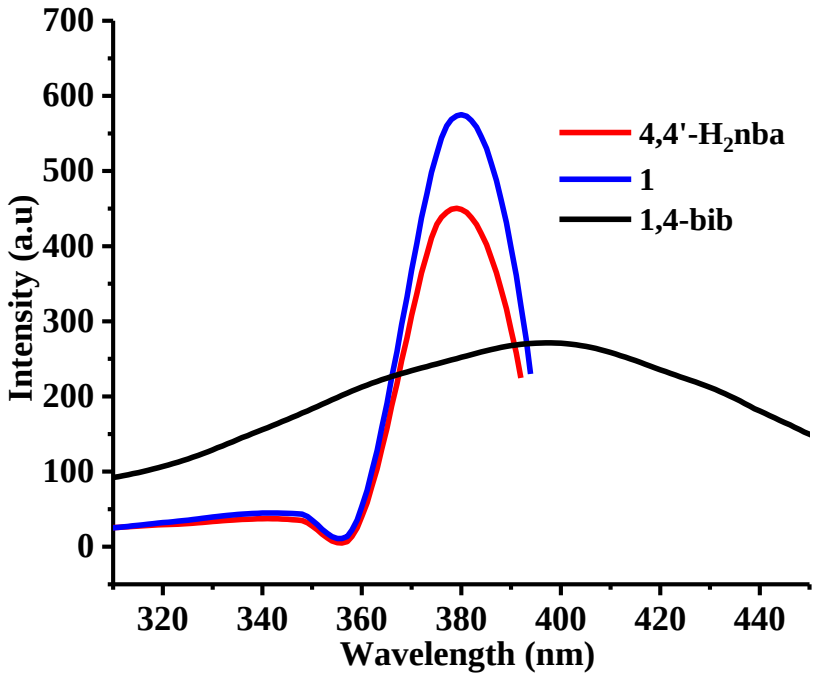

(a)

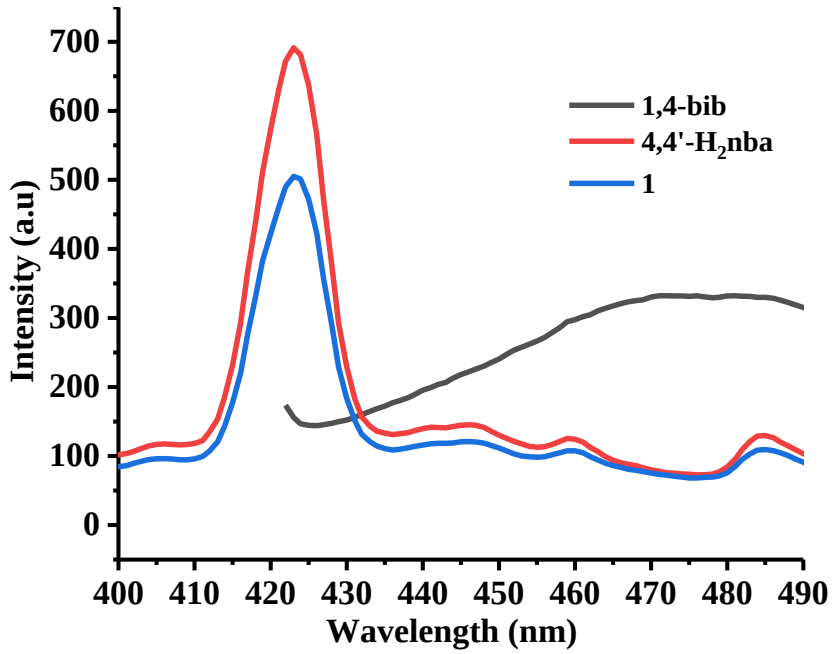

(b)

Figure S4. (a) The solid-state excitation spectra of 4,4′-H_2nba, 1,4-bib and **1** at room temperature, (b) the solid-stateemission spectra of 4,4′-H_2nba, 1,4-bib and **1** at room temperature.

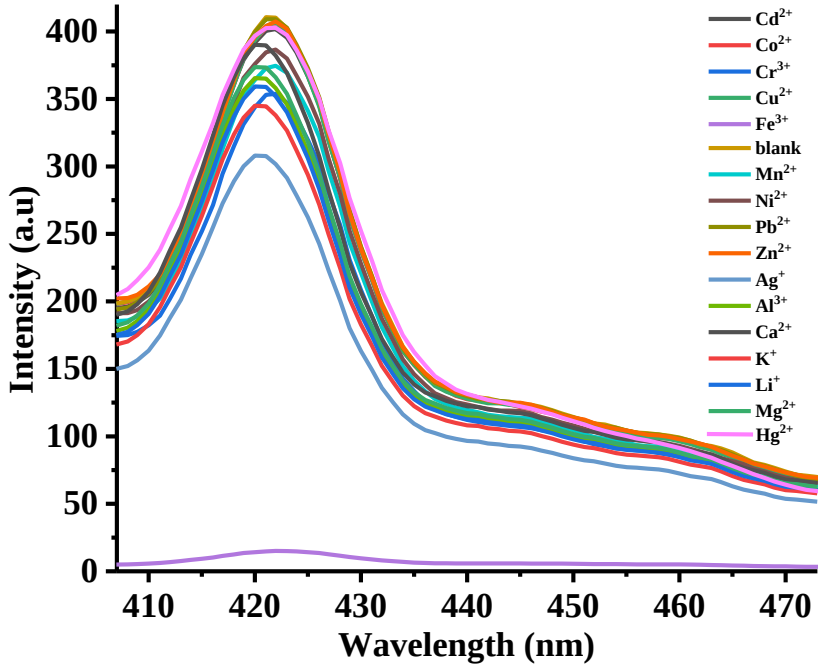

Figure S5. The photoluminescence spectra for **1** in aqurous solution with various inorganic cations.

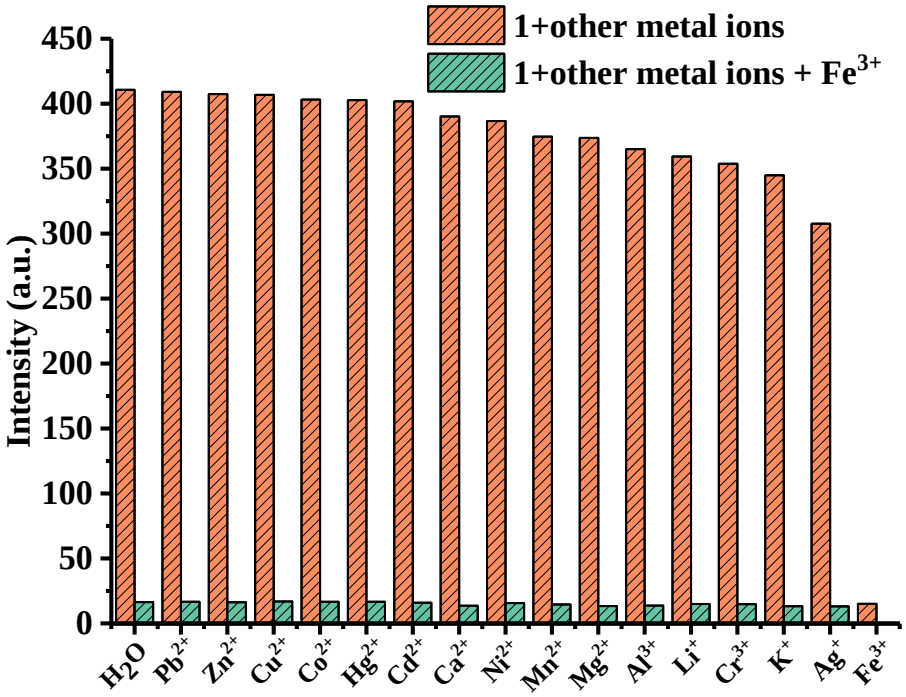

Figure S6. Fluorescence intensity of **1** in aqueous solution with the introduction of diverse other metal ions (organe) and introduction of Fe(III) (green).

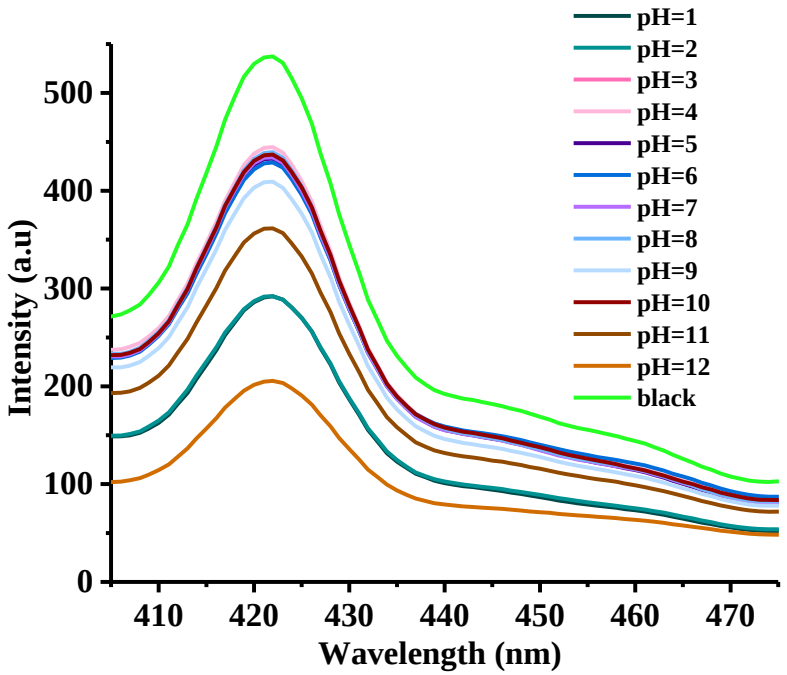

(a)

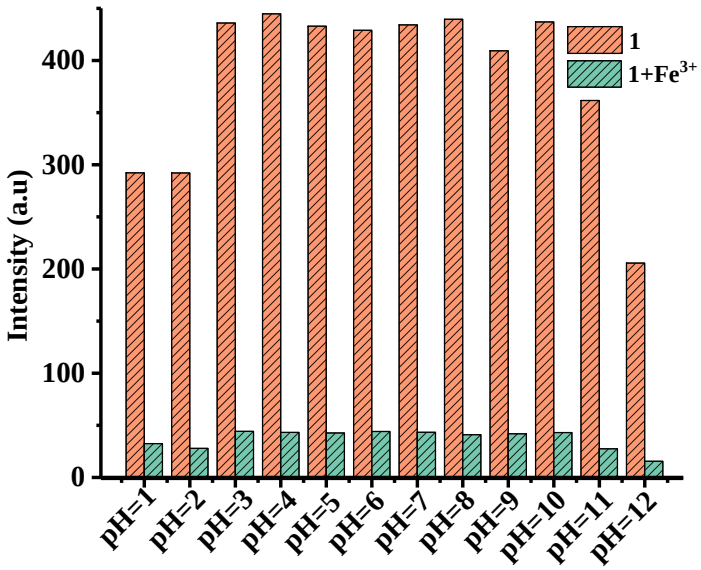

(b)

Figure S7. (a) Emission spectra of **1** for different pH. (b) Fluorescence intensity of **1** in different pH aqueous solution with the unintroduction ions (orange) and introduction of Fe(III) (green).

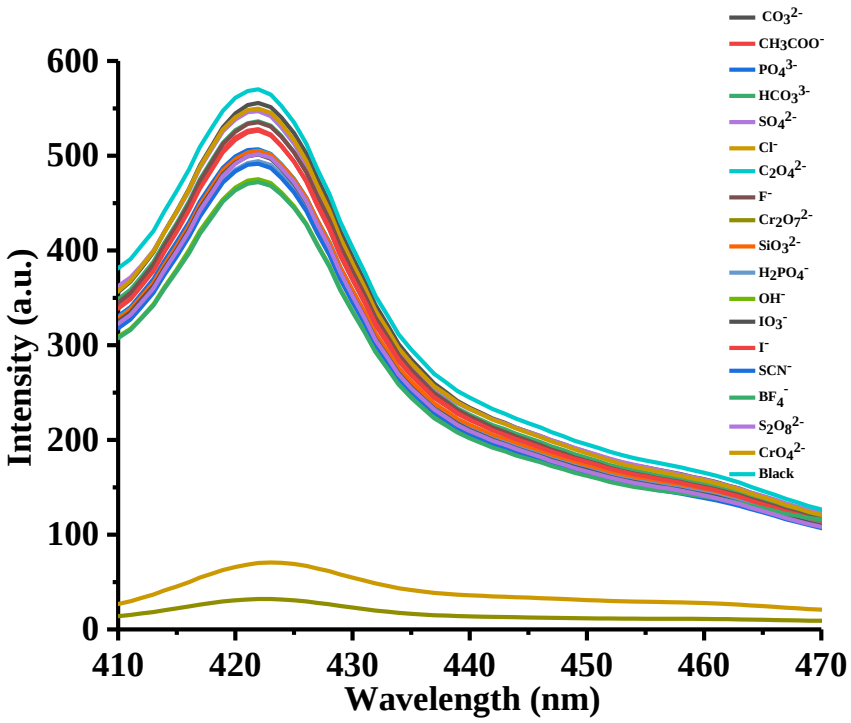

Figure S8. The photoluminescence spectra for **1** in aqurous solution with various anion.

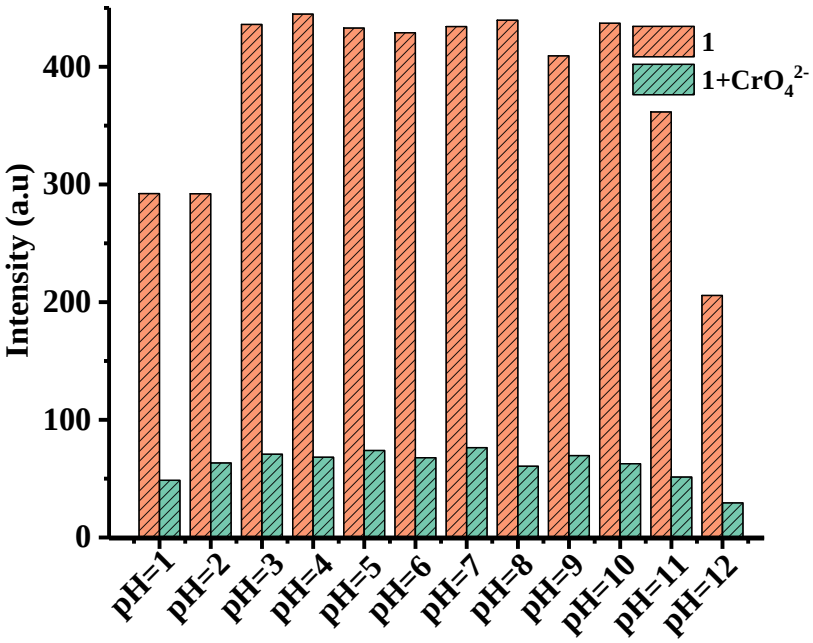

(a)

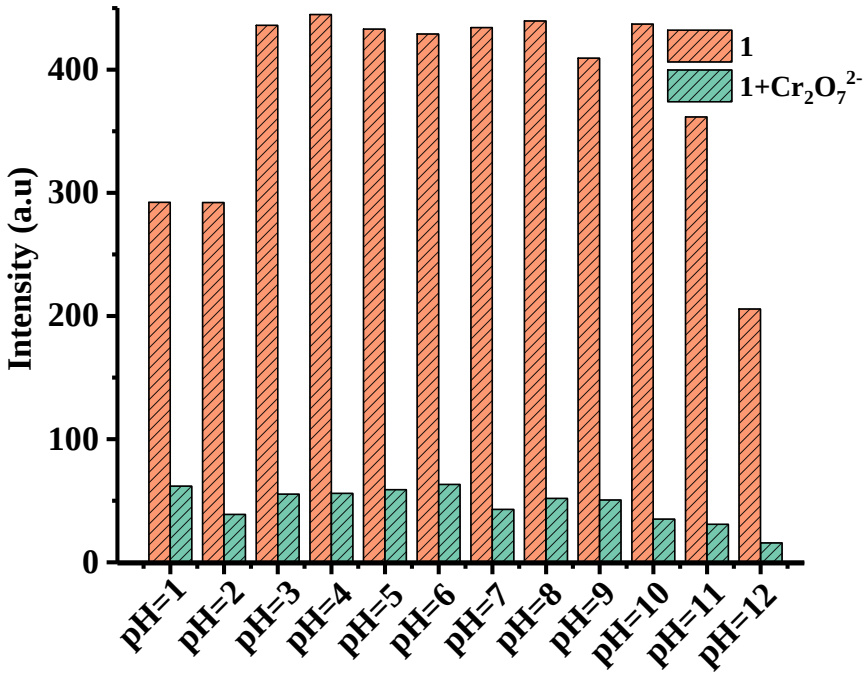

(b)

Figure S9. (a) Fluorescence intensity of **1** in different pH aqueous solution with the unintroduction ions (orange) and introduction of CrO_4^{2-} (green).(b) Fluorescence intensity of **1** in different pH aqueous solution with the unintroduction ions (orange) and introduction of $Cr_2O_7^{2-}$.

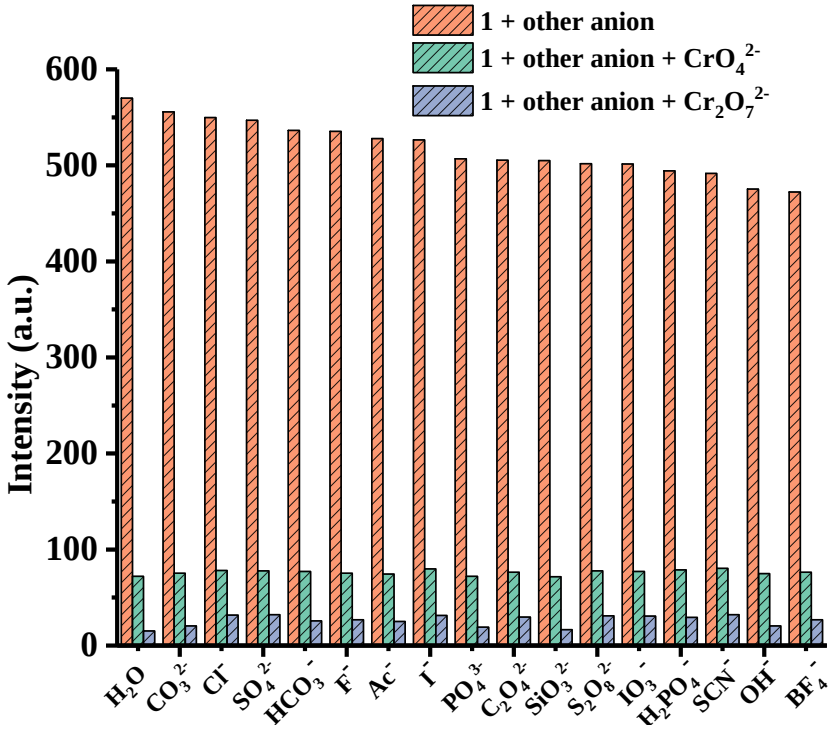

Figure S10. Comparison test fluorescence intensity of **1**.

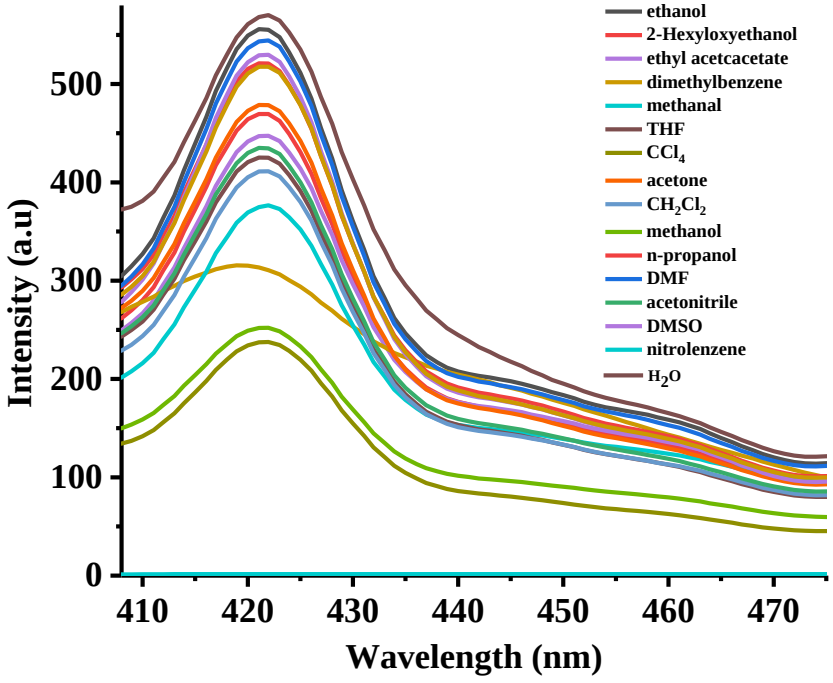

Figure S11. Emission spectra of **1** in diverse organic solvents.

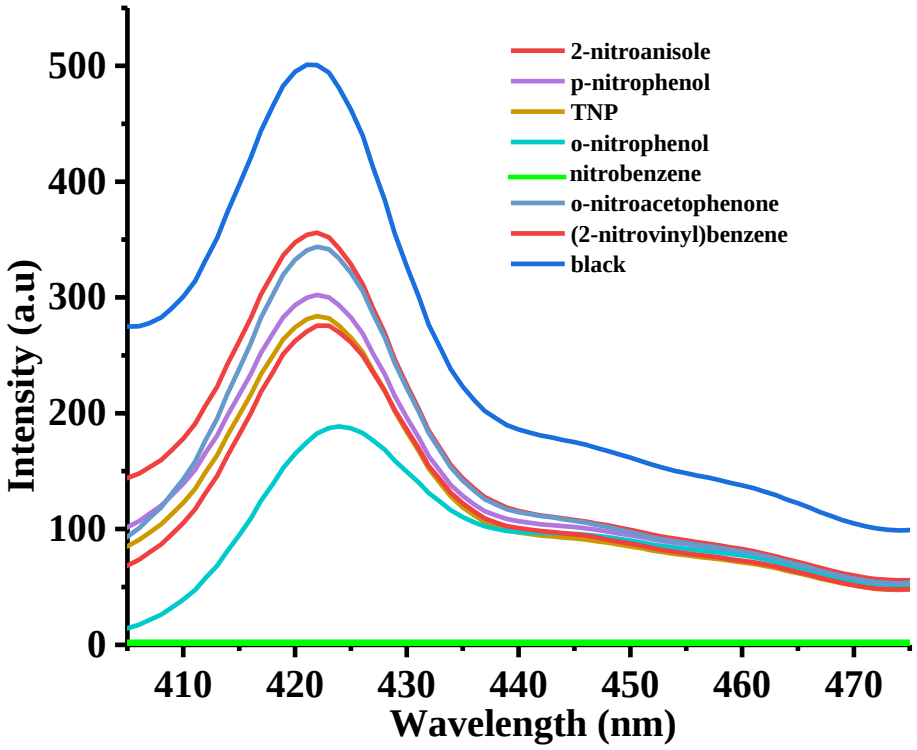

Figure S12. Emission spectra of **1** for nitroaromatic compounds in ethanol.

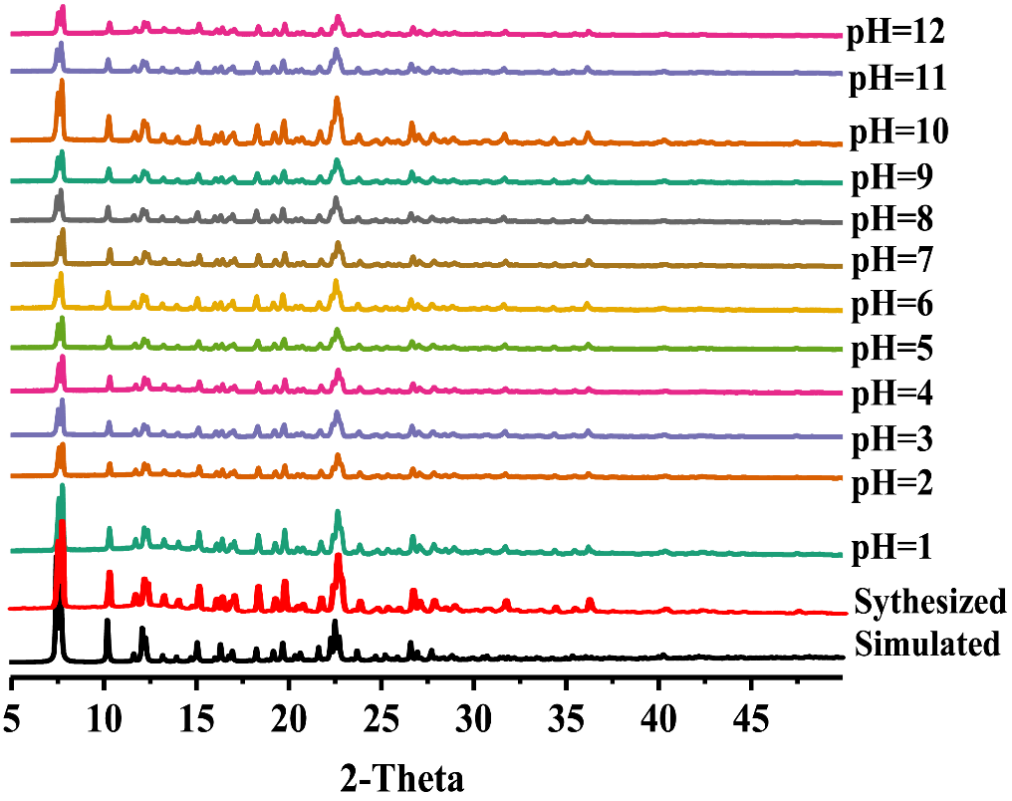

Figure S13. The PXRD patterns of **1** after immersing in aqueous solution at pH = 1-12.

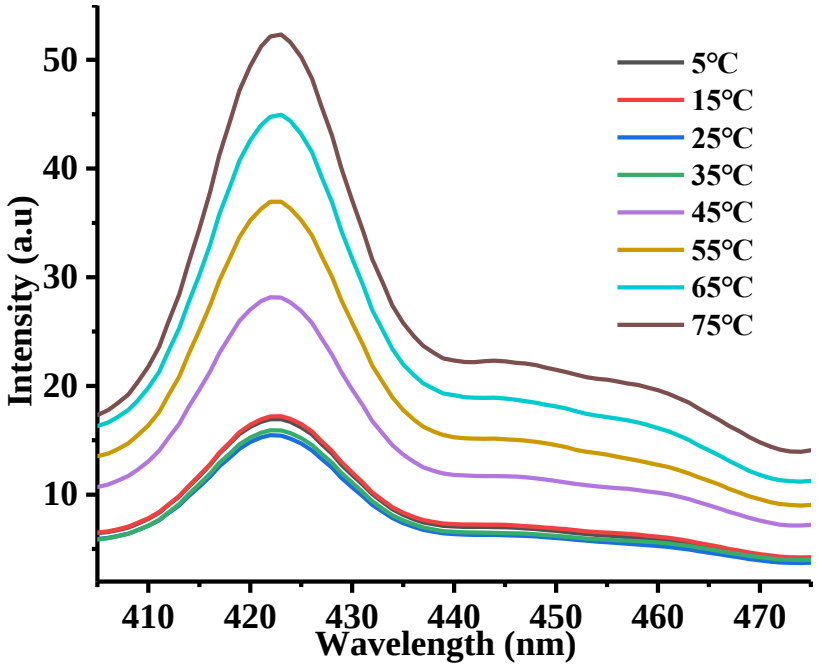
Intensity (a.u)
Wavelength (nm)
5°C
15°C
25°C
35°C
45°C
55°C
65°C
75°C

(a)

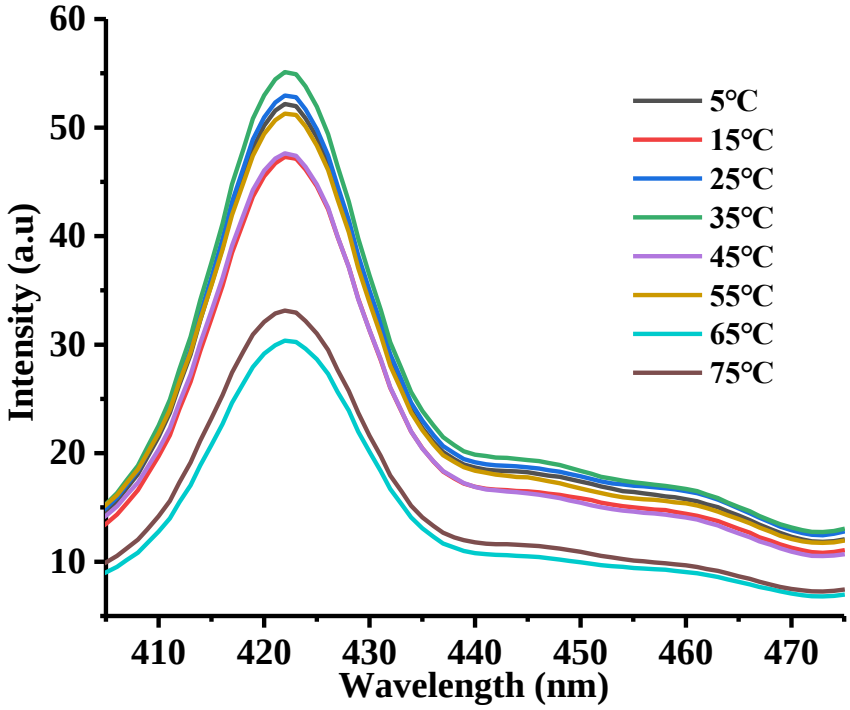
Intensity (a.u)
Wavelength (nm)
5°C
15°C
25°C
35°C
45°C
55°C
65°C
75°C

(b)

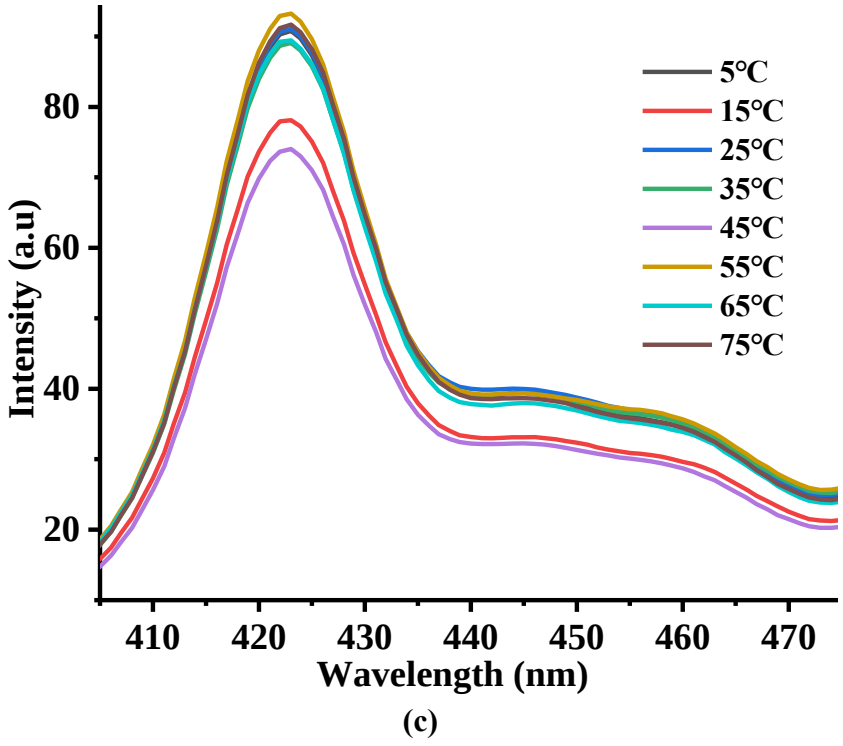

Figure S14. The luminescence emission spectra (a) for **1**@Fe^{3+}, (b) for **1**@$Cr_2O_7^{2-}$ and (c) for **1**@CrO_4^{2-} in aqueous solution at different tempertaure.

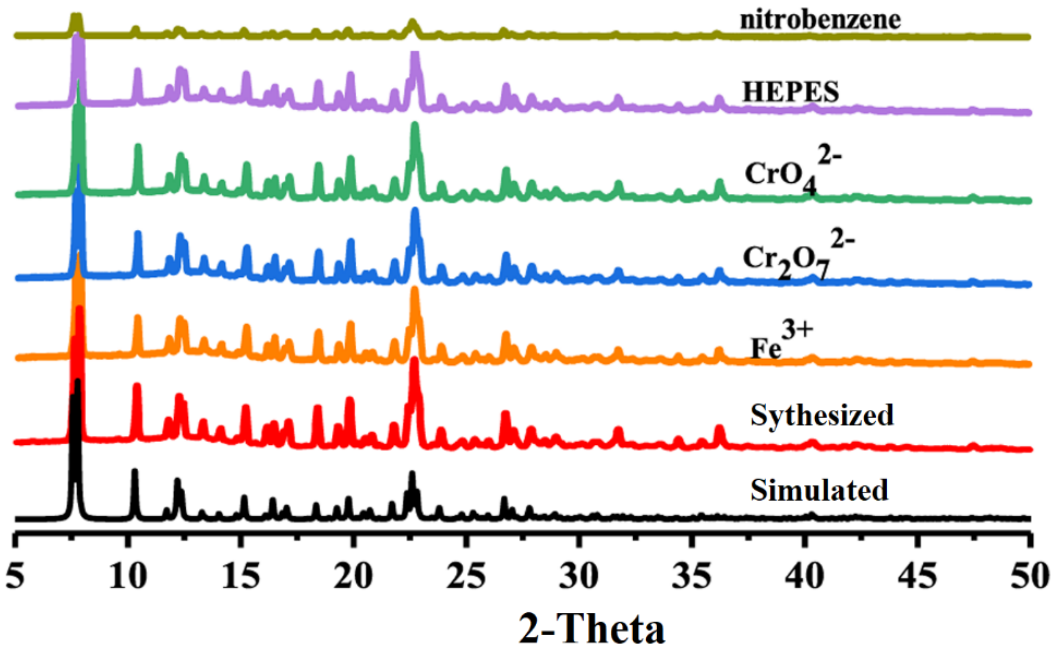

Figure S15. The PXRD profiles of the as-synthesized **1** and the simulated result as reference as well as luminescence sensing analytes.

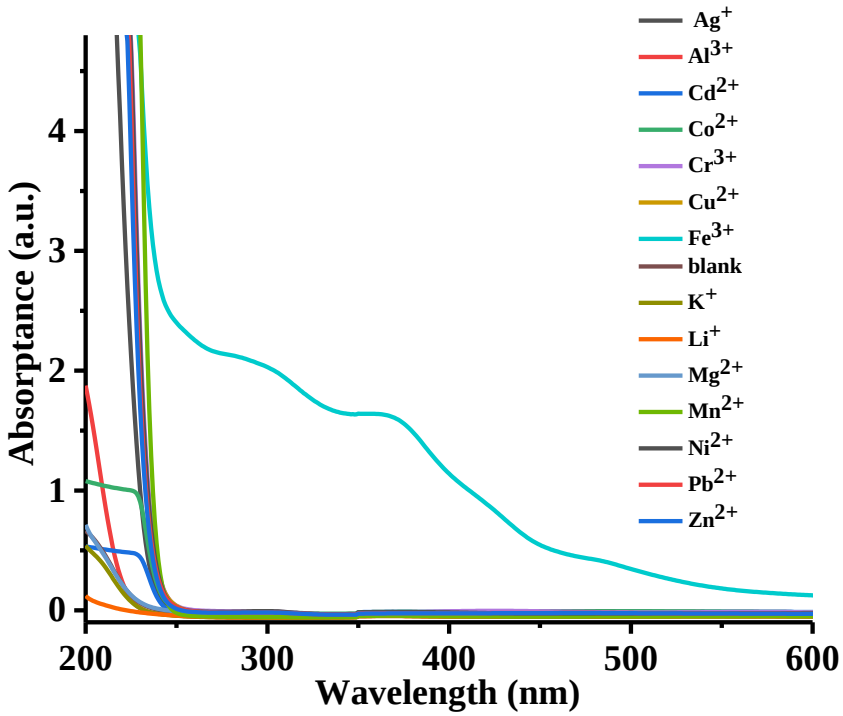
Absorptance (a.u.)
Wavelength (nm)
0
1
2
3
4
200
300
400
500
600
Ag+
Al3+
Cd2+
Co2+
Cr3+
Cu2+
Fe3+
blank
K+
Li+
Mg2+
Mn2+
Ni2+
Pb2+
Zn2+

(a)

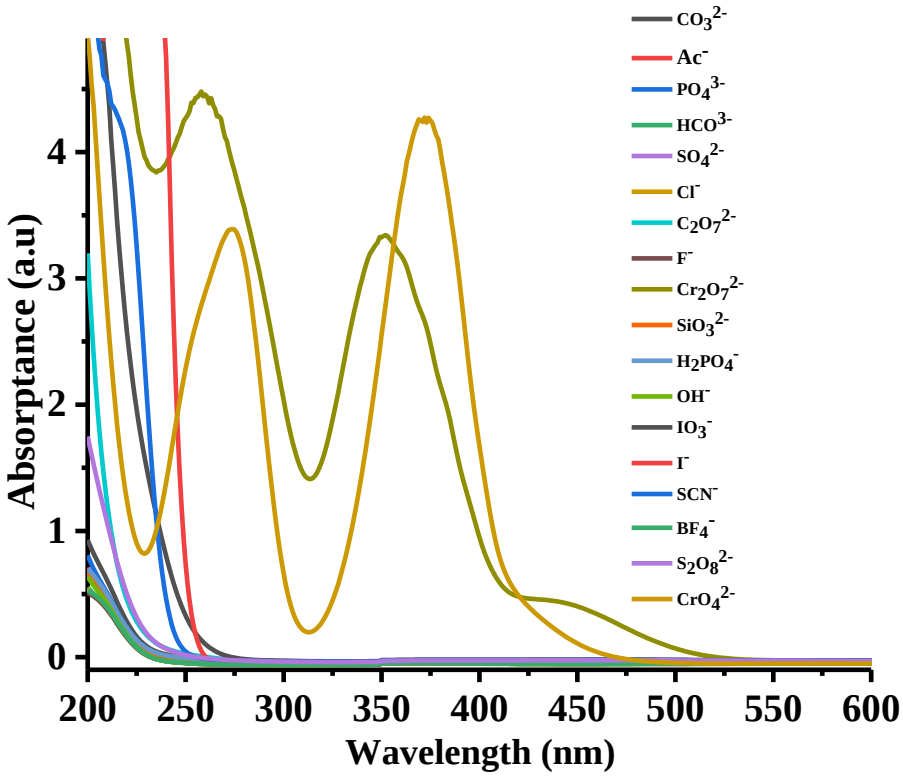
Absorptance (a.u)
Wavelength (nm)
0
1
2
3
4
200
250
300
350
400
450
500
550
600
CO3 2-
Ac-
PO4 3-
HCO3-
SO4 2-
Cl-
C2O7 2-
F-
Cr2O7 2-
SiO3 2-
H2PO4-
OH-
IO3-
I-
SCN-
BF4-
S2O8 2-
CrO4 2-

(b)

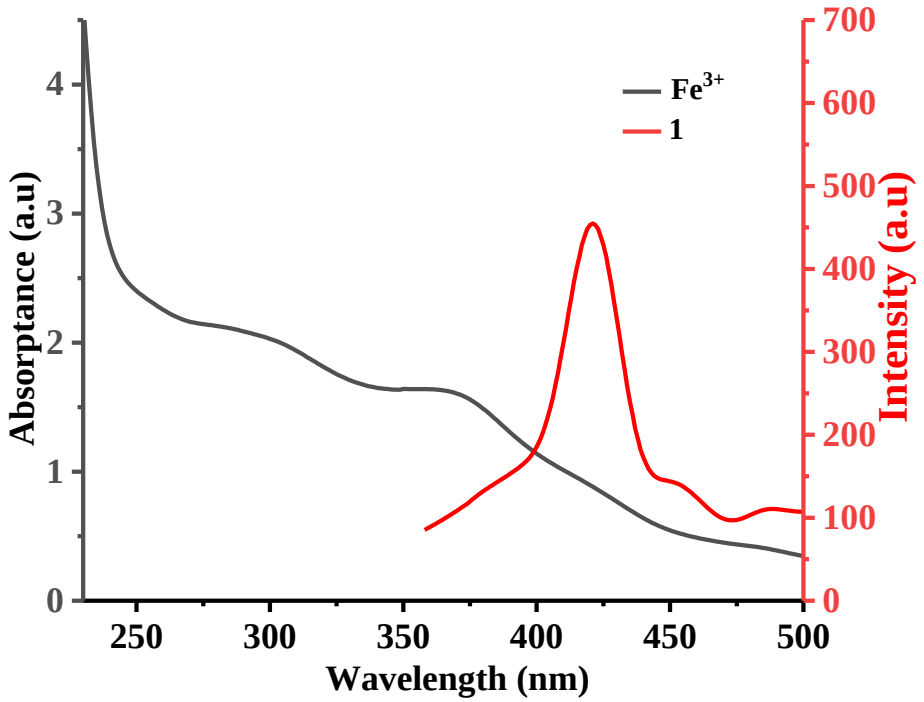

(c)

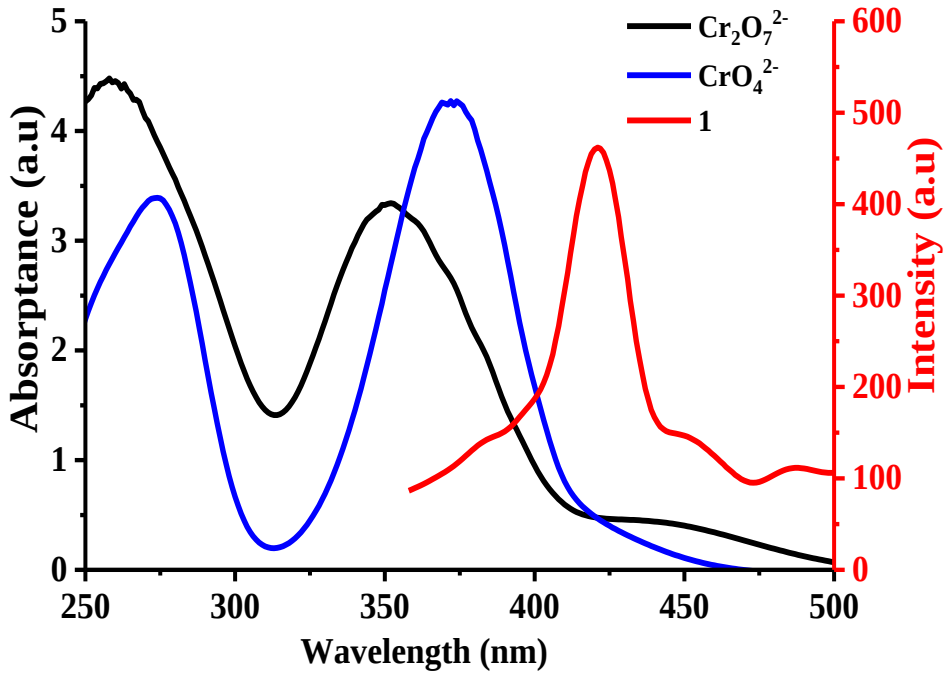

(d)

Figure S16. (a), (b), (c) and (d) Liquid UV-Vis spectra of various anions and emission spectra of **1** in aqueous solution.

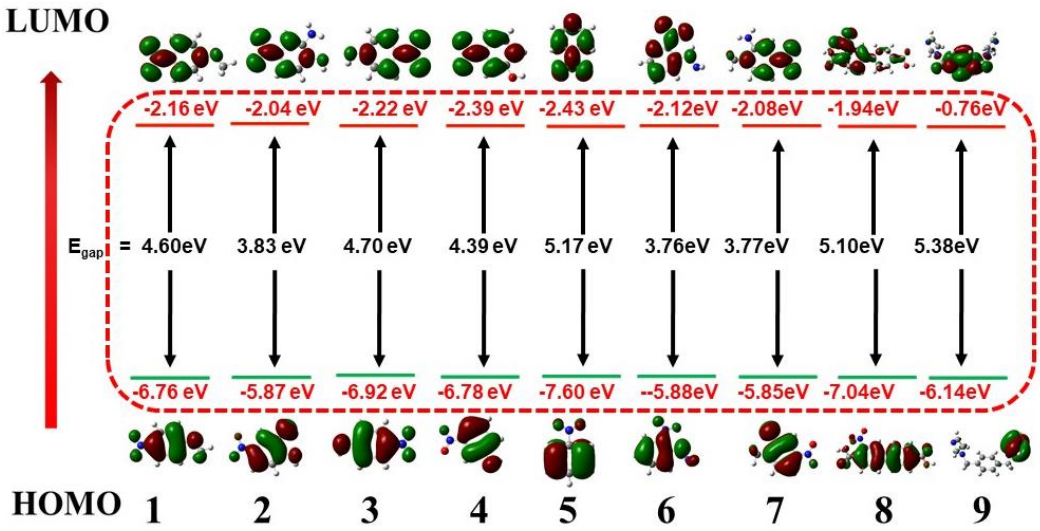

Figure S17. HOMO and LUMO energies (eV) for the selected nitroaromatic compounds and ligands (1: 2-nitroanisole, 2: p-nitrophenol , 3: TNP, 4:o-nitrophenol, 5: nitrobenzene, 6: o-nitroacetophenone, 7: (2-nitrovinyl)benzene, 8: 4,4'-H_2nba, 9: 1,4-bib).

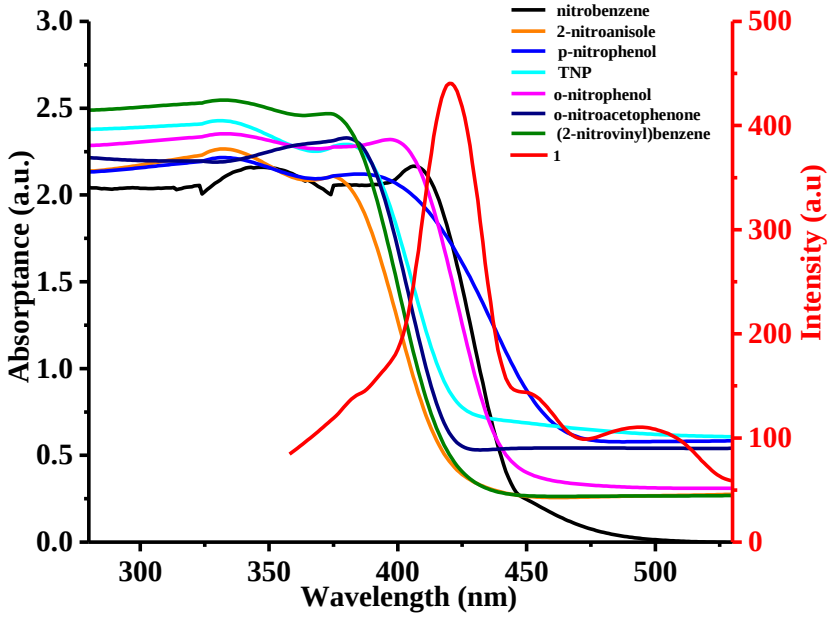

Figure S18. Spectral overlap between normalized absorbance spectra of explosive analytes and the normalized emission spectra of **1** in ethanol.

References:

1 Y. Kang, X. J. Zheng, L. P. Jin, *J. Colloid Interface Sci*. 2016, **471**, 1-6.

2 Y.-N. Wang, H.-X. Li, L. Jia, S.-S. Zhang, Y.-R. Zhao, L. Du, Q.-H. Zhao, *Inorg. Chem. Commun*., 2019, **110**, 107575.

3 F. Zhao, X. Y. Guo, Z. P. Dong, Z. L. Liu, Y. Q. Wang, *Dalton Trans*., 2018, **47**, 8972-8982.

4 X.-L. Zhao, D. Tian, Q. Gao, H.-W. Sun, J. Xu, X.-H. Bu, Dalton Trans., 2016, **45**, 1040-1046.

5 M. Wang, J. G. Wang, W. Xue, A. Wu, *Dyes. Pigments.*, 2013, **97**, 475-480.

6 H. Xie, H. Wang, Z. Xu, R. Qiao, X. Wang, X. Wang, L. Wu, H. Lu, S. Feng, *J. Mater. Chem. C*, 2014, **2**, 9425-9430.

7 Y.-T. Yan, J. Liu, G.-P. Yang, F. Zhang, Y.-K. Fan, W.-Y. Zhang, Y.-Y. Wang, *CrystEngComm*, 2018, **20**, 477-486.

8. M. Guo, Z.-M. Sun, *J. Mater. Chem.*, 2012, **22**,15939-15946.

9 Y.-P. Xia, Y.-W. Li, D.-C. Li, Q.-X. Yao, Y.-C. Du, J.-M. Dou, *CrystEngComm*, 2015, **17**, 2459-2463.

10 L. Yang, C. Lian, X. Li, Y. Han, L. Yang, T. Cai, C. Shao, *Acs. Appl. Mater. Inter.,* 2017, **9**, 17208-17217.

11 Y. Bai, Y. B. Dou, L. H. Xie, W. Rutledge, J.R. Li, H. C. Zhou, *Chem. Soc. Rev*. 2016, **45**, 2327-2367.

12 L. Li, Q. Chen, Z. G. Niu, X. H. Zhou, T. Yang, W. Huang, *J. Mater. Chem. C*, 2016, **4**, 1900-1905.